International Journal of Modern Physics B
Vol. 24, No. 17 (2010) 3269–3295

DOI: 10.1142/S0217979210056025

World Scientific
www.worldscientific.com

VORTICES IN BRAIN WAVES

WALTER J. FREEMAN

Department of Molecular and Cell Biology,
University of California, Berkeley CA 94720-3206 USA
dfreeman@berkeley.edu
http://sulcus.berkeley.edu

GIUSEPPE VITIELLO

Dipartimento di Matematica e Informatica,
and Istituto Nazionale di Fisica Nucleare,
Università di Salerno, I-84100 Salerno, Italy
vitiello@sa.infn.it
http://www.sa.infn.it/giuseppe.vitiello

Received 21 June 2010

Interactions by mutual excitation in neural populations in human and animal brains create a mesoscopic order parameter that is recorded in brain waves (electroencephalogram, EEG). Spatially and spectrally distributed oscillations are imposed on the background activity by inhibitory feedback in the gamma range (30–80 Hz). Beats recur at theta rates (3–7 Hz), at which the order parameter transiently approaches zero and microscopic activity becomes disordered. After these null spikes, the order parameter resurges and initiates a frame bearing a mesoscopic spatial pattern of gamma amplitude modulation that governs the microscopic activity, and that is correlated with behavior. The brain waves also reveal a spatial pattern of phase modulation in the form of a cone. Using the formalism of the dissipative many-body model of brain, we describe the null spike as a singularity, the following amplitude pattern as a ground state, and the phase cone as the manifestation of a stabilizing vortex.

Keywords: Vortex; brain waves; dissipative many-body model of brain.

1. Introduction

The brain in human beings and other animals alike provides the agency for engagement of the body with the environment. Success in guidance and control requires constant search with the several senses, acquisition of information about the current status of the body with respect to its surround, recall at each moment in condensed form of relevant past experience, and rapid recognition of momentary changes to which the body must be accommodated. These operations are not done with logic and mathematics. As observed by von Neumann, "brains lack the arithmetic and logical depth that characterize our computations. We require exquisite numerical precision over many logical steps to achieve what brains accomplish in very few

short steps".[1] The first such step in an act of perception is transduction at sensory receptors of microscopic energies from the surround to represent their information in nerve impulses (action potentials), the common currency of the brain. The second step is transmission to the brain and refinement in the several sensory systems of the requisite information by various well-known analog operations of information pre-processing. The third step is abstraction and generalization to a category of equivalent inputs. The fourth step is incorporation of the information with the knowledge base (memory) in the brain that constructs the meaning for the subject.

These four operations are dynamical processes that begin the "few short steps" of the action-perception cycle by which a brain accommodates itself and the body to the ever-changing, not fully predictable environment.

The neural mechanisms of the first two steps are understood in terms of the construction of microscopic neural networks and Hebbian neural assemblies by mechanisms of growth and learning. The action potentials from arrays of sensory receptors are delivered to cortex by axons organized in topographic maps, which preserve the spatial relations among receptors.

The neural mechanisms of the third and fourth steps are mesoscopic, because they require the formation of nonlocal, very large-scale statistical ensembles. The problem was clearly stated over fifty years ago: "Generalization is one of the primitive basic functions of organized nervous tissue. Here is the dilemma. Nerve impulses are transmitted ... from cell to cell through definite intercellular connections. Yet all behavior seems to be determined by masses of excitation. ... What sort of nervous organization might be capable of responding to a pattern of excitation without limited specialized paths of conduction? The problem is almost universal in the activities of the nervous system".[2]

The third and fourth of the "few short steps" occur in the sensory cortices after they receive the information from receptors. In this report we take up the challenge of describing the "sort of organization" that performs the mass actions and creates the dynamic patterns by which cortices perform them.

It has been shown[3,4] that the dissipative quantum field theory (many-body) model of brain is able to predict two main features of neurophysiological data: the coexistence of physically distinct amplitude modulated (AM) and phase modulated (PM) neuronal patterns correlated with categories of conditioned stimuli and the remarkably rapid onset of AM patterns into irreversible sequences that resemble cinematographic frames. These features of the brain activity are observed in laboratory by means of imaging of scalp potentials (electroencephalograms, EEGs) and of cortical surface potentials (electrocorticograms, ECoGs) of animal and human beings from high-density electrode arrays. The mesoscopic neural activity of neocortex appears indeed consisting of the dynamical formation of spatially extended neuronal domains in which widespread cooperation supports brief epochs of patterned synchronized oscillations, which have been demonstrated to occur in the 12–80 Hz range (β and γ ranges). They re-synchronize in frames at frame rates in the 3–12 Hz range (θ and α ranges).[3,5–8] These patterns, or "packets of waves",

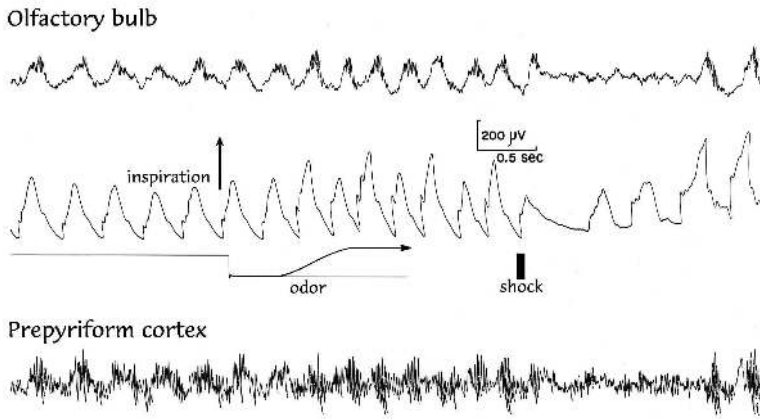

Fig. 1. Bursts of oscillation in olfactory ECoGs require inhalation (upward in middle trace) at time windows determined by the limbic system. The precise time of onset of each frame is determined by the emergence of a null spike.

appear often to extend over spatial domains covering much of the hemisphere in rabbits and cats[9,10] (Fig. 1), from Ref. 19 having linear dimensions up to 19 cm[5] in human cortex with near zero phase dispersion.[11,12] Synchronized oscillation of large-scale neuronal assemblies in β and γ ranges have been detected also by magnetoencephalographic (MEG) imaging in the resting state and in motor task-related states of the human brain.[13] The patterns of phase-locked oscillations are intermittently present in resting, awake subjects as well as in the same subject actively engaged in cognitive tasks requiring interaction with environment, so they are best described as properties of the background activity of brains that is modulated upon engagement with the surrounding.

The observed cortical collective activity cannot be accounted for neither by the electric field of the extracellular dendritic current nor by the extracellular magnetic field from the high-density electric current inside the dendritic shafts, which are much too weak, nor by the chemical diffusion, which is much too slow.[3,14] On the contrary, it turns out that the dissipative many-body model[15] is able to account for the dynamical formation of synchronized neuronal oscillations.[3,4] A brief summary of the dissipative model is reported in the Appendix A (for a detailed discussion see Refs. 3, 4 and 15). Here we only recall that each AM pattern is described to be consequent to spontaneous breakdown of symmetry triggered by external stimulus[15–18] and is associated with one of the quantum field theory (QFT) unitarily inequivalent ground states.[3,15] Their sequencing is associated to the non-unitary time evolution implied by dissipation.[3,15]

In this paper, we focus our attention on a crucial neural mechanism, that has been deduced from experimental observations of a pattern called "Coordinated Analytic Phase Differences" (CAPD),[6–10] consisting in the fact that the event that

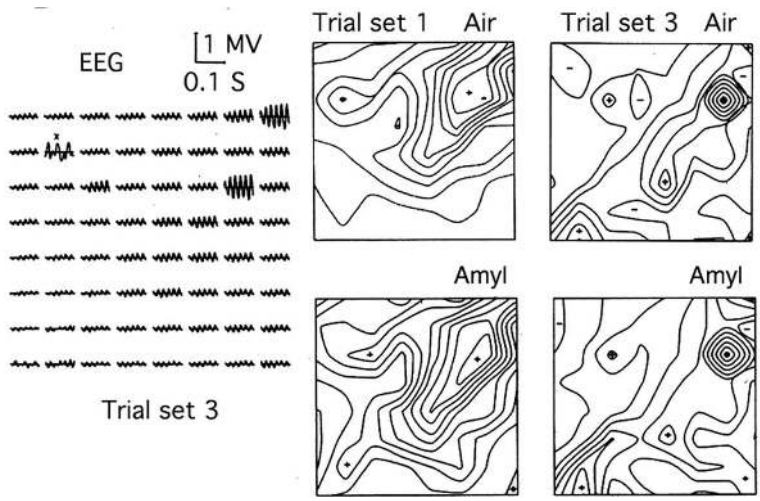

Fig. 2. Left: The burst of gamma oscillation illustrates the amplitude modulation of the shared carrier wave. Right: AM patterns are compared with and without the CS present in the inhaled air. The change between trial sets illustrates consolidation: "off-line" learning requiring participation of the genome.

initiates the transition to a perceptual state is an abrupt decrease in the analytic power of the background activity to near zero, depicted as a *null spike*,[19] associated with the concomitant increase of spatial variance of analytic phase and a discontinuity in space and time of the analytic phase.

Experimental evidence of CAPD over large cortical areas indicates that the neuronal correlation length would cover an entire cerebral hemisphere very quickly (practically without delay in the gamma activity), if measured at the critical transition. Between the null spikes the cortical dynamics is (nearly) stationary for ∼60–160 ms. This is called a frame. The transitions by which they form vary in duration and sometimes are shorter by an order of magnitude.

In Sec. 2 we summarize the formation and the properties of imploding and exploding conical phase gradients and the occurrence of null spikes that have been identified in multichannel records of ECoG signals.[20] In Sec. 3 we discuss phase transitions and vortex solutions in the model and show how energy dissipation incorporates the observed feature of null spikes. There we derive classical Maxwell equations and current fields from the quantum dynamics.[3] We stress that the emergence of classicality out of the microscopic dynamics is a central feature of the dissipative many-body model. We also discuss the size, number and time dependence of the transient non-homogeneous patterns of percepts appearing during non-instantaneous phase transitions, such as those observed in the brain. The formation of imploding and exploding conical phase gradients in the ECoG is shown to be allowed, as indeed deduced from observations. Energy dissipation as heat in the disappearance and emergence of coherence is emphasized in Sec. 4. On the one

hand, brains dissipate metabolic energy at rates 10-fold greater than rates in any other organ, so indirect measures of the rates of dissipation (blood flow, oxygen depletion) are a major resource in brain imaging.[21] On the other hand, dissipation enables brains to form an indefinite variety of differing ground states,[4,15–18] which is prerequisite for high memory capacity. Section 5 is devoted to final remarks and conclusions. Mathematical details and a brief summary of the formalism of the many-body model are presented for completeness in the Appendices A and B.

2. Observations of Patterns Comprising Percepts

The carrier wave has a spatial pattern of phase modulation (PM) pattern[22] having the shape of a cone on the cortical surface (Fig. 3, left, from Ref. 22). The location and sign of the apex are fixed in a frame, but they vary randomly from each frame to the next with no relation to categories of conditioned stimuli. The cone demarcates the abrupt onset and gradual ending of a wave packet. The phase gradient in radians/m (slope of the cone) also varies randomly between frames. Within the frame the phase velocity in m/s (given by the ratio of the carrier frequency, in radians/s, to the phase gradient) is invariant and equals the conduction velocity of the intracortical axons running parallel to the surface.[22,23] The direction of the gradient is either negative (outward from maximum lead at the apex, explosion) or positive (inward from maximum lag at the apex, implosion). Cinematographic display of the amplitudes of the filtered ECoG[24] often shows rotation either clockwise or counterclockwise (Fig. 4, from Ref. 19), giving the appearance of a vortex such as a hurricane seen from a satellite. This suggests that AM patterns are manifestations of a continuous mesoscopic field of activity.[22]

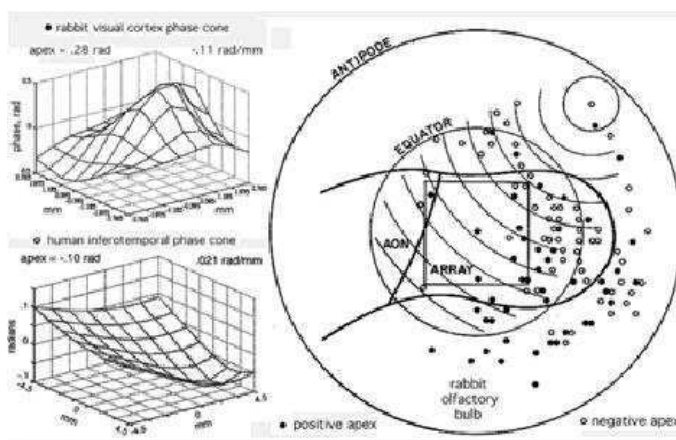

Fig. 3. Left: Examples of phase cones fitted to gamma phase averaged over a frame, referenced to the spatial mean phase after filtering and unwrapping. Right: Silhouette of the olfactory bulb with square array window, with the near-spherical surface flattened to show the random distribution of apices (○ denote phase lead, explosion, negative gradient; ● denote phase lag, implosion, positive gradient).

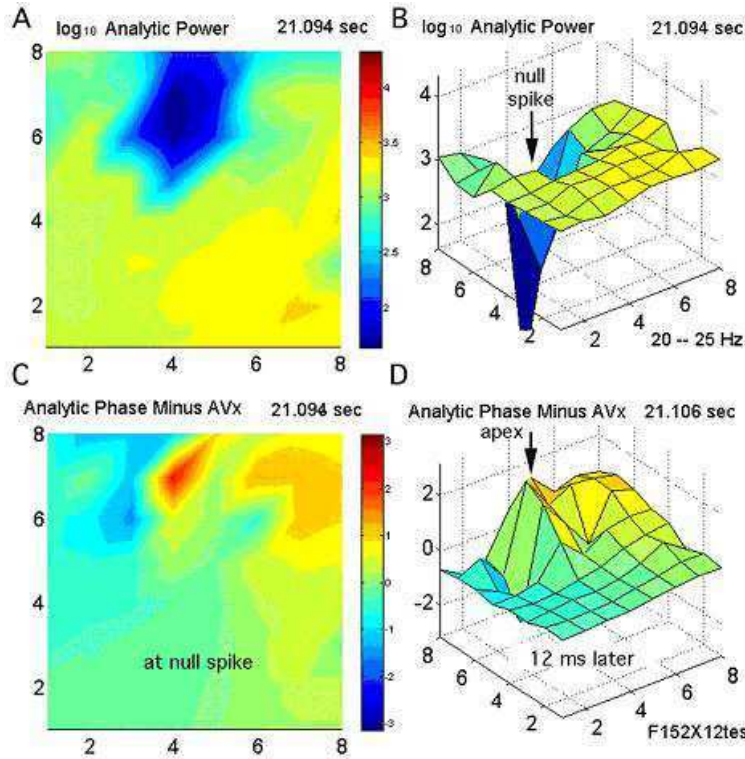

Fig. 4. A. Color-coded contour plot of analytic power (square of amplitude) showing a null spike. B. Perspective view. C. Color-coded plot of analytic phase referenced to spatial average showing phase discontinuity at the site of the null spike. D. Apex of a stable phase cone (sampled 12 ms later) is near the site of the null spike; its negative phase gradient shows the residue of an explosion that occurred in the first quarter cycle after the null spike.

During periods of high amplitude the spatial deviation of phase (SD_X) is low and the phase spatial mean tends to be constant within frames and to change suddenly between frames, indicating coherence and CAPD. The reduction in the amplitude of the spontaneous background activity induces a brief state of indeterminacy in which the power in a significant pass band of the ECoG is near zero and the phase of ECoG is undefined.

Null spikes are observed by band pass filtering the ECoG, applying the Hilbert transform to get the analytic power and taking the logarithm (Fig. 5). The spikes form clusters in time but are not precisely synchronized. One of these null spikes coincides with phase transitions leading to emergence of AM patterns. The analytic frequency, $\Delta\phi(t)/\Delta t$ in rad/sec (Δt = digitizing step), is undefined at and near the cusp, giving high spatial and temporal variance. The null spikes tend to recur aperiodically at rates in the theta (3–7 Hz) ranges, which exemplifies the widely observed cross-spectral linkage of theta and gamma oscillations.[6,25] The theoretical constant of proportionality (0.641[26]) between the null spike repetition rate and

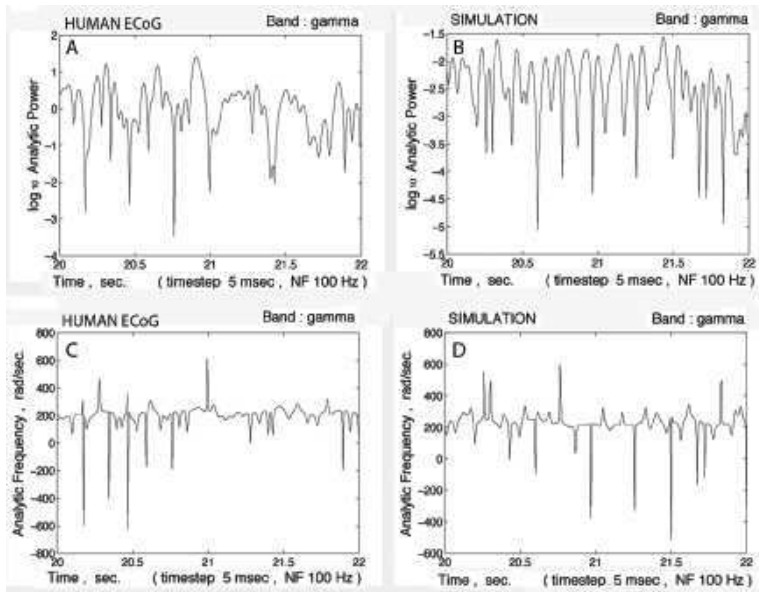

Fig. 5. The temporal patterns of null spikes are illustrated; each spike initiates a spatial phase cone. A. The logarithm of the analytic power (four ECoG signals superimposed from an 8×8 array) in the gamma range (25–50 Hz) shows the downward null spikes demarcating onsets of cones at irregular intervals. C. The spikes in analytic phase coincide with the null spikes in power; the differences between signals reflect the high spatial variance contributed by the cones. B. The statistical properties of null spikes are replicated by cumulatively summing Gaussian noise and applying to the signal the same band pass filter (1/4 to 1/2 the Nyquist frequency, 100 Hz). D. The spikes in analytic phase coincide with the null spikes in power.

the band width of the filter (as measured by the temporal minimum of the spatial standard deviation SD_X in each frame[25]) enables us to predict the bandwidth of the resting gamma (25–50 Hz) in human ECoG with strong alpha waves (8–12 Hz) to be $\sim$13–19 Hz. By use of the Hilbert transform, the local structure of CAPD is visualized in the real and imaginary parts, $a(x)$ and $b(x)$, respectively, of the ECoG sampled wave function $\psi(x)$ in the selected spectral pass band

$$\psi(x) = \mathbf{A}^2(x)e^{i\phi(x)}\,, \tag{1}$$

where $x \equiv (x, y, t)$ in the two surface dimensions of cortex (3 dimensions for the microscopic level of networks), and the analytic power $\mathbf{A}^2(x)$ and the analytic phase $\phi(x)$ are

$$\mathbf{A}^2(x) = \sqrt{a^2(x) + b^2(x)}\,, \quad \phi(x) = \arctan\frac{b(x)}{a(x)}\,, \tag{2}$$

respectively. $\mathbf{A}^2(x)$ forms a feature vector that describes the AM pattern and therefore serves as our order parameter.[3,4] It vanishes at $r(x) = 0$, with $r^2(x) = a^2(x) + b^2(x)$, where, as the second relation in (2) shows, a singularity occurs and

where the phase $\phi(x)$ is obviously undefined. The meaning of this is not purely geometric, but, as we show below, it is intimately related to the microscopic dynamics in the many-body model.

The cortex can be driven across such a "phase transition" to a new AM pattern by the stimulus arriving just before the onset of a null spike (accounting for the unpredictable variation in latency of AM patterns with respect to times of CS onset). The observed velocity of spread of phase transition is finite, i.e., there is no "instantaneous" phase transition; it is determined by the conduction velocities of axons of intracortical neurons, not those of the input axons.

The extreme localization of the null spike in both time and space indicates the existence of a *singularity* in the cortical dynamics, which was predicted by piecewise linearization of the core set of nonlinear ordinary differential equations (summarized in Chap. 6, Fig. 6.30, p. 388 in Ref. 23). The coincidence of the fixed location of the apex of the following phase cone with the location of the preceding null spike indicates that the null spike mediates or precipitates a phase transition, by which a new wave packet forms with an AM pattern that is selected by the sustained activity of a Hebbian assembly triggered by a CS.[25]

3. Phase Transitions, Vortex Solutions and Null Spikes

In this and in the following sections, we focus on describing, in the formalism of the dissipative model, the observed dynamic formation of singularities and vortices in brain waves and the occurrence of phase cones.

As already observed in Sec. 2, cinematographic display of the amplitudes of the filtered ECoG[24] often shows clockwise or counterclockwise rotation, giving the appearance of a vortex. The vortex occupies the whole area of the phase-locked neural activity of the cortex beginning at a point in time and space. Such a vortex is of dynamical origin and may be comparable to the dynamic pattern that is postulated[27] to be the origin of the anatomical vortices of connections that are observed in maps of orientation across visual cortex.

In the process of non-instantaneous phase transitions (as those observed in the brain, indeed), the dissipative model predicts the existence of singularities associated (at the phase cone apex) with the abrupt decrease (null spike) of the order parameter (the feature vector specifying the spatial AM pattern of the analytic amplitude) and the concomitant increase of spatial variance of the phase field (the analytic phase).

To see how singularities appear in the model, we recall that spontaneous breakdown of the global gauge symmetry (see Appendix A) related to the electrical dipoles of water and other molecules[15] implies the existence of collective fields (or modes, or particles), which in QFT are called the Nambu–Goldstone (NG) boson modes[28–30,32–34] (see Appendix A), say $P(x)$ and $P^{\dagger}(x)$. The system ground state is obtained as a coherent condensate of these NG boson modes.[33,34] Let $\mathcal{P} = \rho\delta$ be the non-vanishing polarization density, where ρ and δ are the charge density and

the (average) dipole length. We then write the charge density wave function $\sigma(x)$ as

$$\sigma(x) = \sqrt{\rho(x)}e^{i\theta(x)}\,, \tag{3}$$

with real $\rho(x)$ and $\theta(x)$. The phase $\theta(x)$ is the NG boson field associated with the breakdown of phase symmetry under the global gauge transformation, $\sigma(x) \to e^{i\lambda}\sigma(x)$, $A_\mu(x) \to A_\mu(x)$, where $A_\mu(x)$ is the electromagnetic (e.m.) field and λ is space-time independent. The condition which expresses the symmetry breakdown is the non-vanishing expectation value of the charge density $\rho(x)$ in the system ground state (the vacuum) $|0\rangle$: $\langle 0|\rho(x)|0\rangle = v \neq 0$.

The system is also invariant under the local gauge transformation

$$\sigma(x) \to e^{ie_0\lambda(x)}\sigma(x)\,, \quad A_\mu(x) \to A_\mu(x) + \partial_\mu\lambda(x)\,, \tag{4}$$

where $\lambda(x) \to 0$ for $|x_0| \to \infty$ and/or $|\mathbf{x}| \to \infty$ and the Lorentz gauge, $\partial_\mu A^\mu(x) = 0$, is used. The field equations for A_μ is

$$-\partial^2 A_\mu(x) = j_\mu(x) - \partial_\mu\theta(x)\,, \tag{5}$$

with $j_\mu(x)$ denoting the current. The crucial point is that a shift in the $\theta(x)$ phase field describes the formation of coherent domains of finite size,[35–37] or, stated in different words, non-homogeneous boson condensation of the field $\theta(x)$ in the system ground state. Such a condensation process is thus described by the shift or field translation transformation

$$\theta(x) \to \theta(x) - \alpha f(x)\,, \tag{6}$$

where α is a constant. $f(x)$ is a function, called the boson condensation function, satisfying the same equation satisfied by the $\theta(x)$ field, i.e., $\partial^2 f(x) = 0$. $f(x)$ acts as a "form factor" specific for the considered domain.[37,39–41]

On the one hand, in order for the condensation process to be physically detectable, $f(x)$ has to carry some topological singularity,[35–37] i.e., $f(x)$ has to be path-dependent (see Appendix A). On the other hand, since observables may be influenced by gradients in the boson condensate, $\partial_\mu f(x)$ is related with observables and therefore it has to be single-valued. Moreover, as a result of the single-valuedness of $\sigma(x)$, the topological singularity is characterized by the winding number n: $\oint \nabla f(x) \cdot dl = 2\pi n$, $n = 0, \pm 1, \pm 2, \ldots$, when the integration is performed along the closed circle $(0, 2\pi)$ (flux quantization).

We thus reach the conclusion that the dissipative model describes the appearance of singularities in the basic dynamical processes. Consistently with this scenario, one can also show[37,40,41] that phase transitions can only be induced by a singular boson transformation function $f(x)$. This is the reason why topologically non-trivial extended objects, such as vortices, appear in the processes of phase transitions.[37,40,41] This means that phase transitions driven by boson transformations are always associated with some singularities in the field phase.

In the following subsection we show, indeed, that a regular function $f(x)$ produces a condensation that can be easily "gauged" away by a convenient field transformation, namely gradients in the phase induced by a regular $f(x)$ do not produce any observable effect.

3.1. *Singularities and emergence of classicality*

A crucial feature of our approach consists in the possibility to derive mesoscopic/macroscopic dynamical properties of the system from the many-body dynamics: classicality is thus not derived as the model "classical limit" approximation. Rather, it appears that the system classical behavior cannot be explained without recourse to the underlying many-body dynamics. The classical Maxwell equation for a massive e.m. field, whose discussion in the frame of the dissipative model is briefly summarized in the Appendix A, is[33–36]

$$(\partial^2 + m_V^2)a_\mu(x) = \frac{m_V^2}{e_0}\partial_\mu f(x)\,. \tag{7}$$

Here, $a_\mu(x)$ denotes the massive classical e.m. vector potential. The classical ground state current $j_{\mu,cl}(x)$ turns out to be

$$j_{\mu,cl}(x) = m_V^2\left[a_\mu(x) - \frac{1}{e_0}\partial_\mu f(x)\right], \tag{8}$$

where $m_V^2 \equiv Z_3 Z^{-1}(e_0 v)^2$, with Z_3 and Z wave function renormalization constants and e_0 the electron charge. We have $\partial^\mu j_{\mu,cl}(x) = 0$. The term $m_V^2 a_\mu(x)$ is called the *Meissner current*, while $(m_V^2/e_0)\partial_\mu f(x)$ is the *boson current*.

The mesoscopic field and current are thus given in terms of the boson transformation function. Note that the classical current is related with $\partial_\mu f(x)$, i.e., with variations in the boson transformation function.

From (7) we obtain $a_\mu(x) = (1/\partial^2 + m_V^2)\partial_\mu f(x)$. When $f(x)$ is regular, this gives $\partial^2 a_\mu(x) = 0$ since $\partial^2 f(x) = 0$. Thus Eq. (7) implies $a_\mu(x) = (1/e_0)\partial_\mu f(x)$ for regular $f(x)$, which in turn implies zero classical field ($F_{\mu\nu}(x) = \partial_\mu a_\nu(x) - \partial_\nu a_\mu(x) = 0$) and zero classical current ($j_{\mu,cl}(x) = 0$) since the Meissner and the boson current cancel each other. It is indeed well-known[42] that the gauge field vanishes in the ordered domain region where the order parameter is non-zero. On the contrary, the gauge field is non-zero in the regions where $f(x)$ presents nontrivial topological singularities such as line singularities, e.g., on the line $r = 0$ in the core of a vortex: we have there the "normal" (disordered) state rather than the ordered one and the non-vanishing massive gauge field there propagates (the Anderson–Higgs–Kibble mechanism).[42–44] On the boundaries between the normal and the ordered regions the phase field gradients are non-zero. Instead they are zero in the normal region, e.g., in the vortex core.

We observe that, consistently with observations, the initial site where nonhomogeneous condensation starts (the phase cone apex) is not conditioned by the incoming stimulus, but is randomly determined by the concurrence of a number

of local conditions, such as where the null spike is lowest and the background input is highest, in which the cortex finds itself at the transition process time. The apex is not initiated within frames, but between frames (during phase transitions). The null spike height is randomly determined by interference in the endogenous Rayleigh noise; the input is randomly determined by the environment. In the case of phase symmetry summarized above, the stationary function $f(x)$ solution of our problem may carry a vortex singularity given by

$$f(x) = \arctan\left(\frac{x_2}{x_1}\right) . \tag{9}$$

Equation (9) shows that the phase is undefined on the line $r = 0$, with $r^2 = x_1^2 + x_2^2$, consistently with the observed phase indeterminacy in the process of transition between two AM pattern frames. For a detailed analysis of the vortex properties associated to Eq. (9) see Refs. 35–37. We note that the dissipative model predicts that vortices are initiated during the critical regime of phase transitions, as it is indeed observed, and are observed in the following frames as explosions or implosions with or without rotation.

The null spike appears in the band pass filtered black noise[a] activity and can be conceived as a *shutter* that blanks the intrinsic background ECoG. When the order parameter goes to zero, the microscopic activity (of the background state) does not decrease but, consistently with the model description, it becomes disordered, unstructured (fully symmetric). In such a state of very low analytic amplitude, the analytic phase is undefined, as it is indeed at the center line of the vortex core, and the system, under the incoming weak sensory input, may re-set the background activity in a new AM frame, if any, formed by reorganizing the existing activity, not by the driving of the cortical activity by input (except for the small energy provided by the stimulus that is required to selectively excite a Hebbian nerve cell assembly that is needed to force the phase transition). The analytic amplitude decrease repeats in the theta or alpha range, independently of the repetitive sampling of the environment by limbic input. Consistently with observations, in the dissipative model, the reduction in activity constitutes a singularity in the dynamics at which the phase is undefined. The aperiodic shutter allows opportunities for phase transitions.

Summarizing, singularities are introduced through the condensation function $f(x)$. The spatial gradient of $f(x)$ in the condensate of the $\theta(x)$ phase field accounts for the phase cone which is indeed a spatial phase gradient imposed on the carrier wave of the wave packet. The vortex solution arises as an effect of non-homogeneous condensation of the phase field $\theta(x)$, which spans (almost) the whole system since it is a (quasi-)massless field (it is a collective mode). This explains the fact that

[a]The refractory periods of axons stabilize the background activity by preventing run-away excitation. Their effect is revealed by an increase in the exponent, α, of the power-law spectral density, $1/f^{\alpha}$, above that of brown noise ($\alpha = 2$) to values ranging as high 3 or even 4 giving black noise. See Ref. 45.

in its life-time the vortex is observed to occupy the whole area of the phase-locked neural activity of the cortex.

3.2. *Phase cones and critical regime in the dissipative model*

Transition processes occurring in a finite span of time in which the formation of vortex strings (or other "defects") occurs, have been studied by numerical simulations and theoretical modeling in a number of problems of physical interest.[41,46–48] In these processes, a maximally stable new configuration is attained after a certain lapse of time since the transition has started. The system is said to be in the critical or Ginzburg regime during such a lapse of time. Enough reliable information on the critical regime behavior is provided by using the harmonic approximation for the evolution of the order parameter v, which is now assumed to be space-time dependent (non-homogeneous condensate), $v = v(x,t)$.[40,41,46–48] In general, v depends also on the temperature. However, we will omit the dependence on temperature since this does not affect our discussion and in any case brains homeostatically maintain their temperatures within a very narrow physiological range.

In the harmonic potential approximation of the Ginzburg–Landau formalism in our present brain problem, we expand the $v(x,t)$ field into partial waves, say $u_{\mathbf{k}}(t)$ (see the Appendix B). For each k-mode $u_{\mathbf{k}}(t)$ ($k \equiv \sqrt{\mathbf{k}^2}$), the frequency turns out to be $M_k(t) = \sqrt{\mathbf{k}^2 - m^2(t)}$, with $m(t)$ a parameter[49] (see also Refs. 40, 41 and 50 and the Appendix B). $M_k(t)$ is required to be real for each k at each t. Such a constraint is satisfied during the critical regime time interval provided the relation

$$\mathbf{k}^2 \geq m^2(t)\,, \tag{10}$$

is satisfied for each k-mode at each t. Equation (10) turns out to be a condition on the k-mode propagation. Let $t = 0$ and $t = \tau$ denote the times at which the critical regime starts and ends, respectively. For a given $\mathbf{k}$, Eq. (10) holds up to a time τ_k, provided $m^2(t)$, for $t > \tau_k$, is larger than $\mathbf{k}^2$. The corresponding k-mode can propagate in a span of time $0 \leq t \leq \tau_k$. Thus the "effective causal horizon"[51–53] can happen to be inside the system (possible formation of more than a domain) or outside (single domain formation) according to whether the time occurring to the k-mode to reach the boundaries of the system is longer or shorter than the allowed propagation time, respectively. This determines the dimensions to which the domains can expand.

The value of τ_k is given when the explicit form of $m^2(t)$ is assigned. One may then model the time dependence of $m(t)$[41] in a way to allow vortex formation. One possibility is to choose $m^2(t)$ to be:

$$m^2(t) = m_0^2 e^{2h(t)}\,. \tag{11}$$

The function $h(t)$ is assumed to be monotonically growing in time from $t = 0$ to $t = \tau$. Equation (11) shows that the correlation propagation time is implicitly given

by:

$$h(\tau_k) = \ln\left(\frac{k}{m_0}\right) \propto \ln\left(\frac{L}{\xi}\right) . \tag{12}$$

Here ξ is the correlation length corresponding to the k-mode propagation and $L \propto m_0^{-1}$. L acts as an intrinsic infrared cut-off. Small k values are indeed excluded, due to Eq. (10), by the non-zero minimum value of m^2. Correspondingly, long wavelengths are precluded, i.e., only domains of finite size can be obtained. At the end of the critical regime the correlation may extend over domains of linear size of the order of $\lambda_k \propto m^{-1}(\tau)$.

Our model is further specified by choosing an explicit analytic expression for $h(t)$. When the choice is the one shown in Eq. (B.3) in the Appendix B we have (cf. Eq. (B.4))

$$h(t) \approx \pm\frac{\Gamma}{2}t\,, \tag{13}$$

for $t^2/\tau^2 \approx 1$, with $\Gamma \equiv 1/\lambda\tau_Q$ and λ an arbitrary constant (see Appendix B for the definition of τ_Q).

The number of vortices $n_{\rm def}$ possibly appearing during the critical regime is given in the linear approximation by[41,53]:

$$n_{\rm def} \propto m^2(\tau) \approx m_0^2|\tau/\lambda\tau_Q|\,. \tag{14}$$

We observe that the size of the vortex core is given by $(m(t))^{-1}$ and thus Eqs. (11) and (13) show that such a size evolves in time as $e^{\mp\Gamma t}$, $t < \tau$ ($t < \tau_k$ for the k-mode). This means that we have both, converging (imploding) and diverging (exploding) regimes, as indeed found in laboratory observations of the phase cone behaviors. Since the "normal" state is confined to the vortex core, the shrinking of such a region (imploding regime) may signal that long range correlation, i.e., ordering, is prevailing (the vortex is "squeezed out"); in the opposite case of enlargement of the vortex core (exploding regime), local correlations (disorder) prevail. This agrees with the conclusion reached on the basis of laboratory observations according to which implosion or explosion is obtained if the long axon connections or the local connections predominate, respectively.[54]

Many phase cones show little or no rotation but repetitive outward or inward pulsations with each cycle. When they present rotational gradients (vortices) the singularity is then associated to the vortex core singularity. The model explains all four types of these observed spatiotemporal phase gradients.

We also observe that the negative gradient could be explained in conventional neurodynamics (e.g., in terms of a pacemaker), but not the positive gradient. Also, there is no explanation in the conventional framework of why both gradients, the positive and the negative one, occur, one or the other at random.

4. Heat Dissipation and Disappearence/Emergence of Coherence

We have already commented upon the remarkable interplay between the emergence of the mesoscopic field and currents and the microscopic phenomenon of boson condensation. We further observe that the neural mechanism of perception depends on repeated transfer of mesoscopic energy to microscopic energy and vice-versa, as the basis for the disintegration of a mesoscopic AM pattern and the formation of a new one, respectively. In the dissipative model these energy transfers are controlled by the time derivative of the number N of the NG field condensate[3,15]:

$$dE = \sum_k E_k \frac{dN_k}{dt} dt = \frac{1}{\beta} d\mathcal{S}\,. \tag{15}$$

Equation (15) holds provided changes in the inverse temperature β are slow, which is what actually happens in mammalian brains which keep their temperature nearly constant. It relates the changes in the energy $E \equiv \sum_k E_k \mathcal{N}_k$ and in the entropy $\mathcal{S}$ implied by the minimization of the free energy $\mathcal{F}$ at any t, $d\mathcal{F} = dE - (1/\beta)d\mathcal{S} = 0$ (see Appendix A). In Eq. (15) E_k and $\mathcal{N}_k$ denote the energy and the number of the NG excitations of momentum k. As usual, heat is defined as $dQ = (1/\beta)dS$. We thus see how, through the variations in time of the NG field condensate, the entropy changes and heat dissipation involved in the disappearance/emergence of the coherence (ordering) associated to the AM patterns turns into energy changes. Heat dissipation appears indeed to be a significant variable in laboratory observations. Brains require constant perfusion with arterial blood and venous removal to dispose of substantial waste heat.

Also concerning the mesoscopic/microscopic interplay, it has to be remarked that while the vortex solution in the dissipative model is dynamically generated through the non-homogeneous boson condensation mechanism, which is a truly quantum mechanism, the vortex manifests itself as a solution of non-linear *classical* equations. This is a general feature of QFT, where many kinds of topologically non-trivial solutions of classical field equations (soliton solutions) are described as mesososcopic "envelopes" of microscopic boson condensates (for a detailed discussion on the quantum/classical interplay in field theories with topologically non-trivial solutions see Ref. 55; see also Refs. 35–37 and 56). The dissipative quantum model of brain thus models classical mesoscopic phenomena originating from the underlying quantum dynamics. In such a model the neurons, the glia cells and their subcellular components are *not* quantum objects.[3,4,15] The quantum degrees of freedom are those associated to the dipole vibrational field and to other fields such as the phase field.

5. Final Remarks and Conclusion

As a final comment we remark that Eq. (13) shows that the $\pm$ signs in Eq. (B.3) amount to working with both elements of the basis $(e^{+\Gamma/2t}, e^{-\Gamma/2t})$, as indeed required by mathematical correctness. In this sense, the $\pm$ double sign cannot be

avoided in the model choice of $h(t)$. From a physical point of view, it is equivalent to working with time evolution pointing in one given time direction (say the $t > 0$ arrow of time) and with its "time-reversed" copy or image. This is perfectly consistent with one of the main features of the dissipative model where time-reversed excitations are introduced, thus "doubling" the system degrees of freedom[58,59] (see Appendix A),[b] so that one is led to consider the time-reversed image of the system, its "*Double*". It is interesting that such a model feature finds a connection with the laboratory observation of the exploding/imploding feature in the phase cone behavior.

Our study, which has been based on the mechanism of the spontaneous breakdown of symmetry and on dissipation, has derived several specific predictions from basic dynamical features and compared them directly with experiments. In order to better clarify the theoretical claims and better represent how theory connects with experiments, we list few of the experimentally confirmed predictions of the model. As already mentioned in Sec. 1, in Refs. 3 and 4 we have shown that the model accounts for the observed dynamical formation of spatially extended domains of neuronal synchronized oscillations and of their rapid sequencing. The model explains indeed two main features of the ECoG data:

— the textured patterns of AM in distinct frequency bands correlated with categories of conditioned stimuli, i.e., coexistence of physically distinct AM patterns, and
— the remarkably rapid onset of AM patterns into (irreversible) sequences that resemble cinematographic frames.

Moreover, consistently with experimental observations[5–8,25,60–62] the model predicts that[3,4,63,64]

— very low energy is required to excite AM correlated neuronal patterns,
— AM patterns have large diameters, with respect to the small sizes of the component neurons,
— duration, size and power of AM patterns are decreasing functions of their carrier wave number k,
— there is lack of invariance of AM patterns with invariant stimuli, but constancy with the unchanging meaning of the stimuli.
— there is self-similarity in brain background activity as suggested by power-law distributions of power spectral densities derived from ECoGs data.[60,63,64]

In the present paper, in agreement with experimental observations, we have derived:

— that there is heat dissipation at (almost) constant in time temperature (see also Refs. 3 and 4),
— the occurrence of near-zero down-spikes in phase transitions,

[b]This is quite a general feature of QFT arising in many different contexts. See e.g., Ref. 57.

— the whole phenomenology of occurrence of phase gradients and phase singularities in the vortices formation,
— the constancy of the phase field within the frames,
— the insurgence of a phase singularity associated with the abrupt decrease of the order parameter and the concomitant increase of spatial variance of the phase field,
— the occurrence of phase cones and random variation of sign (implosive and explosive) at the apex,
— that the phase cone apices occur at random spatial locations,
— that the apex is not initiated *within* frames, but *between* frames (during phase transitions).

The model leads to the "classicality" (not derived as the classical limit, but as a dynamical output) of functionally self-regulated and self-organized background activity of the brain. Finally, the model may enable future investigators to predict the number of vortices appearing in the critical regime [cf. Eq. (14)] and the size of the vortex core. Those predictions must await comparisons with experiments in future work, which will require much higher precision of measurement: larger arrays than the present $8 \times 8 = 64$ (e.g., $16 \times 16 = 256$ channels) with the same close spacing of 0.5–0.8 mm; faster digitizing rates that the present 500 Hz (e.g., 2000 Hz with 0.5 msec time step); and clinical mode decomposition of the Hilbert spectrum, together improving the spatial, temporal and spectral resolution of the ECoG and EEG.

We can summarize the whole picture as follows. The foremost problem in studies of perception is to explain how brains seek, presage, and amplify microscopic activity driven by sensory receptors, retrieve and mobilize the relevant prior knowledge about the stimuli, and disseminate the selected knowledge in preparing an appropriate intentional action. Experimental data show that cortex maintains by mutual excitation robust spontaneous background activity that is parsed by inhibitory feedback into oscillations that are both spatially and spectrally distributed. Summation over distributions of beta or gamma frequency ranges gives beats of null spikes at intervals in the theta and alpha frequency ranges. At the minima of these beats the cortex approaches a state of criticality, in which a conditioned stimulus can trigger a micro-to-mesoscopic phase transition in each of the primary sensory cortices, which is asynchronous in the first post-stimulus frame, and which is synchronized globally in following frames. The first phase transition is the gateway to a sequence of transitions toward a macroscopic state of recognition which evolves into the action stage in the action-perception cycle.

The fact that the dissipative many-body model naturally leads to equations describing mesoscopic fields and currents and to soliton-like "classical" solutions (the vortex) (Sec. 3), and to microscopic/mesoscopic thermodynamic interplay (Sec. 4) is certainly a remarkable offspring of the many-body model. The model appears to

provide an efficient way for describing and organizing in a unified and consistent framework a large body of brain function data.

Thus, our approach is not a description of the system in terms of some *ad hoc* classical formalism; it is a direct attack on explaining the link between micro dynamics of neural nets and mesoscopic dynamics of populations that produce observable data structures and patterns.

Finally, we observe that the description of the singularities appearing in the process of phase transitions turns out to be remarkably crucial in the understanding of the nature of the engagement of the subject with the environment in the action-perception cycle. By the continual updating of the meanings of the flows of information exchanged in its relation with the environment, the brain proceeds from information to knowledge in its own world as it is known by itself (Heidegger's Dasein[65]), that we describe as its Double.[56]

Acknowledgments

The authors thank Brian Burke and Bill Redfearn for technical assistance. Partial financial support by INFN and MIUR is also acknowledged.

Appendix A. Basic Features of the Dissipative Many-body Model of Brain

For completeness and for the reader convenience, we summarize here some of the features of the formalism of the dissipative many-body model of brain. A more detailed account of the formalism can be found in Refs. 4, 15, 39–41, 56, 66, 67 and 68.

A.1. *The spontaneous breakdown of symmetry in QFT*

We start by recalling the mechanism of spontaneous breakdown of symmetry in QFT, which describes the occurrence of observable mesoscopic/macroscopic ordered patterns (correlated elements) in physical systems.

Spontaneous breakdown of symmetry occurs when the system dynamics is invariant under a certain group of continuous symmetry, say G, and the system ground state (the vacuum) is not invariant under G, but under one of its subgroups, say G'.[32,37,69] Ordered patterns then appear in the ground state, corresponding to the breakdown of G into G'. These patterns, namely the correlation among the system elementary components, are generated by the coherent condensation in the ground state of massless quanta called Nambu-Goldstone (NG) particles,[30] or waves, or modes, which are the carriers of the ordering information.[37,42] The NG modes are dynamically generated by the process of the breaking of the symmetry and, since their propagation covers extended domains, or, in the infinite volume limit, the whole system, they manifest themselves as collective modes. The degree of ordering

is specified by a mesoscopic/macroscopic (classical) field, called the order parameter, which thus acts as a mesoscopic/macroscopic variable for the system. Its value is related with the density of condensed NG bosons in the vacuum. It may thus be considered to be the *code* specifying the vacuum of the system among many possible degenerate vacua existing in QFT.[32,37,69]

A.2. *The dissipative quantum model of brain*

In the original many-body model of the brain, formulated by Umezawa and collaborators in 1967–1979,[16–18] the code of the ground state specifies its memory content: the NG boson condensation in the brain ground state describes the process of memory recording. The external input acts as the trigger of the breakdown of the rotational symmetry of the electrical dipoles of the water molecules and other biomolecules,[28,29] with consequent appearance of non-vanishing polarization density (for the role played by electric polarization see, for example, the experimental observations[70,71] of slow fluctuations in neuronal membrane polarization, the so-called up and down states). The corresponding NG modes are the vibrational dipole wave quanta (DWQ).[33,34] The recall of the memory occurs under the input of a stimulus "similar" to the one responsible for the memory recording.

The original model does not consider the fact that the brain is a dissipative system, namely an *open system* permanently coupled with environment. This is considered in the dissipative quantum model where the dynamics of the original model is extended so as to include dissipation.[15]

In the study of a dissipative system the flow of the energy exchanged between the system and the environment has to be balanced (energy conservation). This is achieved by "doubling" the degrees of freedom of the system,[58] which also ensures the possibility to perform the canonical quantization.

We denote by A_k ($A_k^\dagger$) the annihilation (creation) operators for the DWQ mode and by $\tilde{A}_k$ ($\tilde{A}_k^\dagger$) its "doubled mode" (representing the environment or thermal bath with which the energy is exchanged). k denotes the momentum and other quantum numbers of the A operators.

Let $\mathcal{N}$ be the *code* imprinted in the vacuum at the initial time $t_0 = 0$ by the external input: it specifies the *memory record* of the input. The code $\mathcal{N}$ is the set of the numbers $\mathcal{N}_{A_k}$ of modes A_k, for any k, condensate in the vacuum state, which we denote by $|0\rangle_{\mathcal{N}}$. This can be taken to be the memory state at $t_0 = 0$.[15,39] At each t, $\mathcal{N}_{A_k}(t)$ is given by:

$$\mathcal{N}_{A_k}(t) \equiv {}_{\mathcal{N}}\langle 0(t)|A_k^\dagger A_k|0(t)\rangle_{\mathcal{N}} = \sinh^2(\Gamma_k t - \theta_k)\,, \tag{A.1}$$

and similarly for the modes $\mathcal{N}_{\tilde{A}_k}(t)$. The state $|0(t)\rangle_{\mathcal{N}} \equiv |0(\theta,t)\rangle$ is the time-evolved of the state $|0\rangle_{\mathcal{N}}$. Γ_k is the damping constant (related to the memory life-time) and θ_k fixes the code value at $t_0 = 0$. $|0\rangle_{\mathcal{N}}$ and $|0(t)\rangle_{\mathcal{N}}$ are normalized to unity and in

the infinite volume limit we have

$$ {}_{\mathcal{N}}\langle 0(t)|0\rangle_{\mathcal{N}'} \underset{V\to\infty}{\longrightarrow} 0 \;\forall\, t \neq t_0\,, \quad \forall\, \mathcal{N}, \mathcal{N}'\,, \tag{A.2} $$

$$ {}_{\mathcal{N}}\langle 0(t)|0(t')\rangle_{\mathcal{N}'} \underset{V\to\infty}{\longrightarrow} 0\,, \quad \forall\, t, t' \text{ with } t \neq t'\,, \quad \forall\, \mathcal{N}, \mathcal{N}'\,, \tag{A.3} $$

with $|0(t)\rangle_{\mathcal{N}'} \equiv |0(\theta', t)\rangle$. Equations (A.2) and (A.3) also hold for $\mathcal{N} \neq \mathcal{N}'$ but $t = t_0$ and $t = t'$, respectively. The meaning of Eqs. (A.2) and (A.3) is that the vacua of the same code $\mathcal{N}$ at different times t and t', for any t and t', and, similarly, at equal times but different $\mathcal{N}$'s, are orthogonal states in the infinite volume limit, $V \to \infty$, and thus the corresponding Hilbert spaces $\{|0(t)\rangle_{\mathcal{N}}\}$ are unitarily inequivalent spaces in the same limit.

In order to ensure the balance of energy flow between the system and the environment, the difference between the number of tilde and non-tilde modes must be zero: $\mathcal{N}_{A_k} - \mathcal{N}_{\tilde{A}_k} = 0$, for any k. We remark that the difference $(\mathcal{N}_{A_k} - \mathcal{N}_{\tilde{A}_k})$ is a constant of motion for any k and θ.

We now observe that the requirement $\mathcal{N}_{A_k} - \mathcal{N}_{\tilde{A}_k} = 0$, for any k, does not uniquely fix the set of $\mathcal{N}_{A_k}$ numbers, i.e., the code $\mathcal{N} \equiv \{\mathcal{N}_{A_k}, \text{for any } k\}$. Indeed, $|0\rangle'_{\mathcal{N}}$ with $\mathcal{N}' \equiv \{\mathcal{N}'_{A_k}; \mathcal{N}'_{A_k} - \mathcal{N}'_{\tilde{A}_k} = 0, \text{ for any } k\}$ also ensures the energy flow balance and therefore also $|0\rangle'_{\mathcal{N}}$ is an available memory state corresponding to a different information (of code $\mathcal{N}'$) than the one of code $\mathcal{N}$. Thus, infinitely many memory (vacuum) states may exist, each one corresponding to a different code $\mathcal{N}$: in the sequential recording process, a huge number of sequentially recorded inputs may coexist *without destructive interference* since infinitely many vacua $|0\rangle_{\mathcal{N}}$, for all $\mathcal{N}$, are *independently* accessible. The "brain (ground) state" is the the superposition of the states $|0\rangle_{\mathcal{N}}$, for all $\mathcal{N}$. The collection of the Hilbert spaces $\{|0(t)\rangle_{\mathcal{N}}\}$, for all $\mathcal{N}$, for all t, is called the *memory space*.

Summarizing, the system $\tilde{A}$ represents the sink (the environment or thermal bath) where the energy dissipated by the A system flows. Due to dissipation, the brain is described as a complex system with a huge number of mesoscopic states (the memory states).

A.3. *The free energy functional*

In order to study the thermal properties of the system, let us consider the free energy functional for the system A (we could consider similar functional for the system $\tilde{A}$)

$$ \mathcal{F}_A \equiv {}_{\mathcal{N}}\langle 0(t)| \left(H_A - \frac{1}{\beta} S_A \right) |0(t)\rangle_{\mathcal{N}}\,. \tag{A.4} $$

Here, $\beta(t) = 1/k_B T(t)$ is the time-dependent inverse temperature; S_A is the entropy operator and H_A denotes the Hamiltonian at $t = t_0$ for the A-modes only, $H_A =$

$\sum_k \hbar\Omega_k(t_0) A_k^\dagger A_k$. Let $\Theta_k \equiv \Gamma_k t - \theta_k$ and $E_k \equiv \hbar\Omega_k(t_0)$. The stationarity condition to be satisfied at each time t by the state $|0(t)\rangle_{\mathcal{N}}$ is

$$\frac{\partial \mathcal{F}_A}{\partial \Theta_k} = 0\,, \quad \forall\ k\,, \tag{A.5}$$

which gives $\beta(t)E_k = -\ln \tanh^2(\Theta_k)$, i.e.,

$$\mathcal{N}_{A_k}(\theta, t) = \sinh^2(\Gamma_k t - \theta_k) = \frac{1}{\mathrm{e}^{\beta(t)E_k} - 1}\,. \tag{A.6}$$

Equation (A.6) is the Bose distribution for A_k at time t.

The entropy $\mathcal{S}_A(t) = \langle 0(t)|S_A|0(t)\rangle_{\mathcal{N}}$ appears to be a decreasing function of time in the interval $(t_0 = 0, \tau \equiv (\theta_k/\Gamma_k))$ (and similarly for the $\mathcal{S}_{\tilde{A}}(t)$): the state $|0(t)\rangle_{\mathcal{N}}$, although evolving in time, is however "protected" from "going back" to the "uncorrelated" vacuum state. Here, the exchange of energy with the environment is crucial and we are also assuming finite volume effects. The entropy, for each of the A and $\tilde{A}$ systems separately, grows monotonically from zero to infinity as the time goes from $t = \tau$ to $t = \infty$. For the complete system $A - \tilde{A}$, the difference $(S_A - S_{\tilde{A}})$ is constant in time: $[S_A - S_{\tilde{A}}, \mathcal{H}'] = 0$.

Moreover, provided variations in time of the inverse temperature are slow, i.e., $(\partial\beta/\partial t) = -(1/k_{\tilde{A}}T^2)(\partial T/\partial t) \approx 0$, the variations of the energy $E_A \equiv \sum_k E_k \mathcal{N}_{A_k}$ and of the entropy are related by Eq. (15) in Sec. 4, which expresses nothing but the minimization of the free energy: $d\mathcal{F}_A = dE_A - (1/\beta)d\mathcal{S}_A = 0$ at each time t.

A.4. *The brain-environment entanglement and chaotic trajectories in the memory space*

The states $|0(t)\rangle_{\mathcal{N}}$, for each $\mathcal{N}$ at each time t, are generalized coherent states of the SU(2) group.[49,58] In these states the modes A_k and $\tilde{A}_k$ are entangled modes, which means that the brain is permanently (and unavoidably) "linked" to its environment.[15,56]

The degree of the coupling of the system A with the system $\tilde{A}$ can be parameterized by an index, say n, in such a way that in the limit of $n \to \infty$ the possibilities of the system A to couple to $\tilde{A}$ are "saturated".[39] Thus n represents the number of *links* between A and $\tilde{A}$. When n is not very large (infinity), the system A (the brain) has not fulfilled its capability to establish links with the external world. More are the links, i.e., more the system is "open" to the external world, better its neuronal correlation can be realized.[39] The realization of these correlations also depend on other *internal* parameters which are characteristic of the system and may parameterize subjective attitudes. However, the dissipative model is not able to provide a dynamics for the variations of n. Thus we cannot predict if n increases or decreases in time. In any case, n provides a measure of a higher or lower *degree of openness* to the external world, producing, under different circumstances, e.g.,

during the sleep or the awake states, the childhood or the older ages, a better or worse ability in setting up neuronal correlates, respectively.

We thus see that in the dissipative model functional or effective connectivity (as opposed to the structural or anatomical one, not considered here) is highly dynamic. Once functional connections are established, they are not necessarily persistent: they may quickly decay and new configurations of connections may be formed among a larger or a smaller number of neurons. The finiteness of the size of correlated neuronal domain implies a non-zero effective mass of the DWQ. These therefore propagate through the domain with a greater inertia than in the case of large (infinite) volume where they are (quasi-)massless. The domain correlations are consequently established with a certain time-delay, which concurs in the delay observed in the recruitment of neurons in a correlated assembly under the action of an external stimulus.

In agreement with observations, we can show that the time derivative of the frequency Ω_k common to the A and $\tilde{A}$ modes, i.e., the power, is a decreasing function of k. Also in agreement with observations, the inverse of Ω_k (the "duration") and the domain size $d_\Omega(t) = c(\Omega_k)^{-1}$ are decreasing functions of k. Here c is the propagation speed of the NG modes in the correlated domain.

Note that in the infinite volume limit time evolution of the state $|0\rangle_{\mathcal{N}}$ is represented as the (continual) transition through the spaces $\{|0(t)\rangle_{\mathcal{N}}, \forall\, \mathcal{N}, \forall\, t\}$, namely as the "trajectory" in the memory space through the "points" $\{|0(t)\rangle_{\mathcal{N}}, \forall\, \mathcal{N}, \forall\, t\}$ (each one minimizing the free energy functional (A.4)). The initial condition of the trajectory at $t_0 = 0$ is specified by the code $\mathcal{N}$. These trajectories can be shown to be classical[49,66–68] chaotic[66] trajectories. They satisfy indeed the requirements characterizing the chaotic behavior:

(i) the trajectories are bounded and each trajectory does not intersect itself (trajectories are not periodic).
(ii) there are no intersections between trajectories specified by different initial conditions.
(iii) trajectories of different initial conditions are diverging trajectories.

The property (i) means that the "points" $|0(t)\rangle_{\mathcal{N}}$ and $|0(t')\rangle_{\mathcal{N}}$ through which the trajectory goes, for any t and t', with $t \neq t'$, after the initial time $t_0 = 0$, never coincide.

Equation (A.3), which also holds for $\mathcal{N} \neq \mathcal{N}'$ in the infinite volume limit for any t and any t', shows that trajectories specified by different initial conditions ($\mathcal{N} \neq \mathcal{N}'$) never cross each other, which is the meaning of (ii). The property (ii) thus implies that no *confusion* (interference) arises among the codes of different neuronal correlates, even as time evolves. We observe that states with different codes may have non–zero overlap (the inner products Eqs. (A.2) and (A.3) are not zero) in realistic situations of finite volume. Then, at a "crossing" point between two, or more than two, trajectories, there can be "ambiguities" in the sense that

one can switch from one of these trajectories to another one which there crosses. This may be felt as an "association of memories", switching from one information to another one; it reminds us of the "mental switch" occurring during the perception of ambiguous figures, or while performing some perceptual and motor tasks as well as while resorting to free associations in memory tasks.

For the property (iii), we study the "distance" between trajectories as time evolves. Consider two trajectories with different initial conditions. From Eq. (A.1) we have at time t, for each component $\mathcal{N}_{A_k}(t)$ of the code $\mathcal{N}$,

$$\begin{aligned}\Delta\mathcal{N}_{A_k}(t) &\equiv \mathcal{N}'_{A_k}(\theta', t) - \mathcal{N}_{A_k}(\theta, t) \\ &= \sinh^2(\Gamma_k t - \theta_k + \delta\theta) - \sinh^2(\Gamma_k t - \theta_k) \approx \sinh(2(\Gamma_k t - \theta_k))\delta\theta_k \,, \quad \text{(A.7)}\end{aligned}$$

where $\delta\theta_k \equiv \theta_k - \theta'_k$ (which, in full generality, is assumed to be greater than zero). The last equality holds for small $\delta\theta_k$, i.e., for a very small difference in the initial conditions of the two initial states. The time-derivative then gives

$$\frac{\partial}{\partial t}\Delta\mathcal{N}_{A_k}(t) = 2\Gamma_k \cosh(2(\Gamma_k t - \theta_k))\delta\theta_k \,. \quad \text{(A.8)}$$

thus showing that the difference between originally even slightly different $\mathcal{N}_{A_k}$'s grows as time evolves. For large enough t, the modulus of the difference $\Delta\mathcal{N}_{A_k}(t)$ and its time derivative diverge as $\exp(2\Gamma_k t)$, for all k's. The quantity $2\Gamma_k$, for each k, appears thus to play a role similar to that of the Lyapunov exponent in chaos theory. Summarizing, trajectories differing by a small variation $\delta\theta$ in the initial conditions, diverge exponentially as time evolves. This may account for the high perceptive resolution in the recognition of the perceptual inputs.

Suppose that the difference between *k-components* of the codes $\mathcal{N}$ and $\mathcal{N}'$ becomes zero at a given time $t_k = \theta_k/\Gamma_k$ [cf. Eq. (A.7)]. Then, the difference between the codes $\mathcal{N}$ and $\mathcal{N}'$ does not necessarily become zero. The codes are different even if a finite number of their components are equal, since they are made up of a large number of $\mathcal{N}_{A_k}(\theta, t)$ components (infinite in the continuum limit). On the other hand, suppose that, for $\delta\theta_k \equiv \theta_k - \theta'_k$ very small, the time interval $\Delta t = \tau_{\max} - \tau_{\min}$, with $\tau_{\min}$ and $\tau_{\max}$ the minimum and the maximum, respectively, of $t_k = \theta_k/\Gamma_k$, for *all* k's, be very small. Then the codes are recognized to be *almost* equal in such a Δt. Equation (A.7) then expresses the recognition (or recall) process and it shows how it is possible that "slightly different" $\mathcal{N}_{A_k}$-patterns (or codes) are recognized to be the *same code* even if corresponding to slightly different inputs. Roughly, Δt may be taken as a measure of the recognition time.

The rules (i), (ii) and (iii) are for deterministic chaos, which is low dimensional, noise-free, autonomous and stationary. Such a chaotic motion in the abstract space of the parameters labeling the system ground state must be projected in a more realistic frame considering that brains are infinite dimensional, noisy, engaged and time–varying.

A.5. *Classical behaviors emerging from microscopic dynamics*

The spontaneous breakdown of the dipole rotational symmetry briefly discussed above leads to a non-vanishing polarization density.[33] This means that the system vacuum has a residual cylindrical symmetry along the polarization direction. It is then possible that the spontaneous breakdown of such a residual symmetry (formally represented by the U (1) group of the global gauge transformation) may occur, generating the correspondent NG boson modes.[34] In Sec. 3, these NG modes have been identified with the $\theta(x)$ phase field of the charge density wave function $\sigma(x)$ [cf. Eq. (3)]. The system possesses also the local gauge symmetry [Eq. (4)] and the e.m. field A_μ has the field equation (5).

It is known[35–37] that in the presence of spontaneous breakdown of the global phase symmetry, a massless negative norm field (ghost) $b_{\rm in}(x)$ and a massive vector field $U^\mu(x)$ also exist in the theory and that the NG and the ghost modes do not appear in the physical spectrum (the Anderson–Higgs–Kibble mechanism).[42–44] We denote by $U^\mu_{\rm in}(x)$ the quasi-particle field associated to $U^\mu(x)$. The field equations for $\theta(x)$, $b_{\rm in}(x)$ and $U^\mu_{\rm in}(x)$ are

$$\partial^2\theta(x) = 0\,, \quad \partial^2 b_{\rm in}(x) = 0\,, \tag{A.9}$$

$$(\partial^2 + m_V^2)U^\mu_{\rm in}(x) = 0\,, \quad \partial_\mu U^\mu_{\rm in}(x) = 0\,. \tag{A.10}$$

In these equations $m_V^2 \equiv Z_3 Z^{-1}(e_0 v)^2$, where Z_3 and Z are wave function renormalization constants, e_0 and v are the electron charge and the constant entering the symmetry breakdown condition $\langle 0|\rho(x)|0\rangle = v \neq 0$.[33–37]

Non-homogeneous boson condensation of the field $\theta(x)$ in the system ground state produces coherent domains of finite size. The condensation process is formally described by the transformation (6).[37,39–41] The boson condensation function $f(x)$ carries some topological singularity in order for the condensation process to be physically detectable, which means that it has to be path-dependent,[35–37] i.e., $[\partial_\mu, \partial_\nu]f(x) \neq 0$, for certain μ, ν, x.

We now sketch the general strategy to obtain from the microscopic dynamics the classical Maxwell (massive) field equation and the classical current. The customary requirement that the current $j_\mu(x)$ is the only source of the vector potential field $A_\mu(x)$ in any observable process amounts to impose the so-called physical state condition: ${}_p\langle b|\partial_\mu\theta(x)|a\rangle_p = 0$, i.e., from Eq. (5)

$$-\partial^2\,{}_p\langle b|A^0_\mu(x)|a\rangle_p = {}_p\langle b|j_\mu(x)|a\rangle_p\,, \tag{A.11}$$

where $|a\rangle_p$ and $|b\rangle_p$ denote two generic physical states. Equation (A.11) is the classical Maxwell equation. The physical state condition ${}_p\langle b|\partial_\mu\theta(x)|a\rangle_p = 0$ is violated when the boson transformation (6) is induced and thus the classical Maxwell equation (A.11) is violated. One then can show[35,36] that, in order to restore it, the shift in $\theta(x)$, Eq. (6), must be compensated by means of the transformation of $U^\mu_{\rm in}(x)$:

$$U^\mu_{\rm in}(x) \to U^\mu_{\rm in}(x) + Z_3^{-\frac{1}{2}} a^\mu(x)\,, \quad \partial_\mu a^\mu(x) = 0\,, \tag{A.12}$$

provided the c-number function $a^\mu(x)$ satisfies the equation (7), which is recognized to be the classical Maxwell equation for the massive vector potential $a_\mu(x)$.[33–36]

The various field operators are not affected by (A.12) since they contain $U^\mu_{\rm in}(x)$ and $\theta(x)$ in a combination such that the changes of $\theta(x)$ and of $U^\mu_{\rm in}(x)$ compensate each other. The classical ground state current $j_{\mu,cl}(x)$ turns out to be given by Eq. (8). Remarkably, the classical equation (7) and the classical current (8) are invariant under the classical gauge transformations

$$a_\mu(x) \to a_\mu(x) + \partial_\mu\lambda(x)\,, \quad f(x) \to f(x) + e_0\lambda(x)\,, \tag{A.13}$$

where $\lambda(x)$ is the (non-singular) gauge function satisfying $\partial^2\lambda(x) = 0$.

Appendix B. Ginzburg Regime and Phase Transitions

In the Subsec. 3.B we have considered the critical or Ginzburg regime during the processes of phase transitions in the harmonic approximation formalism. The order parameter classical field v, assumed to be space–time dependent (non-homogeneous condensate), $v = v(x,t)$, is expanded into partial waves:

$$v(x,t) = \sum_{\mathbf{k}} \{u_{\mathbf{k}}(t)e^{i\mathbf{k}\cdot\mathbf{x}} + u^\dagger_{\mathbf{k}}(t)e^{-i\mathbf{k}\cdot\mathbf{x}}\}\,. \tag{B.1}$$

The equations for the parametric oscillators $u_{\mathbf{k}}(t)$[49] (see also Refs. 40 and 41) for each k-mode ($k \equiv \sqrt{\mathbf{k}^2}$) are:

$$\ddot{u}_{\mathbf{k}}(t) + (\mathbf{k}^2 - m^2)u_{\mathbf{k}}(t) = 0\,. \tag{B.2}$$

As remarked in the text, the oscillator frequency $M_k(t) = \sqrt{\mathbf{k}^2 - m^2(t)}$ is required to be real for each k at each t, when m^2 is assumed in the model to depend on time, $m^2 = m^2(t)$. The reality condition on $M_k(t)$ for each k is then satisfied provided at each t, during the critical regime time interval, Eq. (10) is satisfied for each k-mode, which turns out to be a condition on the k-modes propagation. The model is specified by assigning the time dependence of $m(t)$, Eq. (11), and the explicit analytic expression for $h(t)$ which there appears. A possible choice for $h(t)$ is[41]:

$$h(t) = \pm\frac{at}{bt^2 + c}\,, \tag{B.3}$$

where a, b, c are (positive) parameters chosen so as to guarantee the correct dimensions. We denote their ratios by $c/a\lambda \equiv \tau_Q$, $a\lambda/b \equiv \tau_0$, with λ an arbitrary constant. We note that $h(\tau_Q) = h(\tau_0)$. The time derivative of $h(t)$, and thus of $m^2(t)$, is zero at $t = \tau = \pm\sqrt{\tau_Q\tau_0}$. τ thus plays the role of the equilibrium time scale. With this choice Eq. (13) is then obtained

$$h(t) = \pm\frac{1}{\lambda\tau_Q}\frac{1}{1 + \frac{t^2}{\tau^2}}t \approx \pm\frac{\Gamma}{2}t\,, \tag{B.4}$$

for $t^2/\tau^2 \approx 1$, with $\Gamma \equiv 1/\lambda\tau_Q$.

References

1. J. von Neumann, *The Computer and the Brain* (Yale UP, New Haven, CT, 1958), p. 63.
2. K. S. Lashley, *The Problem of Cerebral Organization in Vision*, Biological Symposia VII, Vol. 301, ed. J. Cattell (1942), p. 306.
3. W. J. Freeman and G. Vitiello, *Phys. Life Rev.* **3**, 93 (2006), http://www.arxiv.org/find [Freeman]; q-bio.OT/0511037.
4. W. J. Freeman and G. Vitiello, *J. Phys. A: Math. Theor.* **41**, 304042 (2008), http://Select.iop.org; q-bio.NC/0701053v1.
5. W. J. Freeman, B. C. Burke, M. D. Holmes and S. Vanhatalo, *Clin. Neurophysiol.* **114**, 1055 (2003).
6. W. J. Freeman, B. C. Burke and M. D. Holmes, *Human Brain Mapping* **19**(4), 248 (2003).
7. W. J. Freeman, *Clin. Neurophysiol.* **115**, 2077 (2004); http://repositories.cdlib.org/postprints/1006.
8. W. J. Freeman, *Clin. Neurophysiol.* **115**, 2089 (2004); http://repositories.cdlib.org/postprints/1486.
9. W. J. Freeman, *Clin. Neurophysiol.* **116**(5), 1118 (2005); http://repositories.cdlib.org/postprints/2134.
10. W. J. Freeman, *Clin. Neurophysiol.* **117**(3), 572 (2006); http://repositories.cdlib.org/postprints/1480/.
11. W. J. Freeman, G. Gaál and R. Jornten, *Intern. J. Bifurc. Chaos* **13**, 2845 (2003).
12. W. J. Freeman and L. J. Rogers, *Intern. J. Bifurc. Chaos* **13**, 2867 (2003).
13. D. S. Bassett, A. Meyer-Lindenberg, S. Achard, T. Duke and E. Bullmore, *Proc. Natl. Acad. Sci. USA* **103**, 19518 (2006).
14. W. J. Freeman, *J. Integrative Neuroscience* **4**(4), 407 (2005).
15. G. Vitiello, *Int. J. Mod. Phys. B* **9**, 973 (1995).
16. L. M. Ricciardi and H. Umezawa, *Kibernetik* **4**, 44 (1967).
17. C. I. J. Stuart, Y. Takahashi and H. Umezawa, *J. Theor. Biol.* **71**, 605 (1978).
18. C. I. J. Stuart, Y. Takahashi and H. Umezawa, *Found. Phys.* **9**, 301 (1979).
19. W. J. Freeman and R. Kozma, Freeman's mass action, *Scholarpedia* **5**(1), 8040 (2010); http://www.scholarpedia.org/article/Freeman%27s_mass_action.
20. W. J. Freeman, *How Brains Make Up Their Minds* (Columbia UP, New York, 2001).
21. W. J. Freeman, S. M. Ahlfors and V. Menon, *Intern. J. Psychophysiology* **73**(1), 43 (2009); http://repositories.cdlib.org/postprints/3386.
22. W. J. Freeman and G. Vitiello, *J. Physics Conf Series* **174**, 012011 (2009); http://www.iop.org/EJ/toc/1742-6596/174/1.
23. W. J. Freeman, Frontiers in biology, in *Intelligent Systems*, Part II Brain Components as Elements of Intelligent Function, Vol. 3 (Academic Press, New York, 2001), p. 509.
24. W. J. Freeman, Displays of movies of null spikes resembling tornados and vortices resembling hurricanes can be downloaded from: http://sulcus.berkeley.edu, "Latest Freeman Manuscripts", Section H.
25. W. J. Freeman, *Cognitive Neurodynamics* **3**(1), 105 (2009); http://repositories.cdlib.org/postprints/3387.
26. S. O. Rice, *Mathematical Analysis of Random Noise and Appendixes*, Technical Publications Monograph B-1589 (Bell Telephone Labs Inc., New York, 1950).
27. J. J. Wright, D. M. Alexander and P. D. Bourke, *Vision Research* **46**, 2703 (2006).
28. M. Jibu and K. Yasue, *Quantum Brain Dynamics and Consciousness* (John Benjamins, Amsterdam, 1995).
29. M. Jibu, K. H. Pribram and K. Yasue, *Int. J. Mod. Phys. B* **10**, 1735 (1996).

30. J. Goldstone, *Nuovo Cimento* **19**, 154 (1961).
31. J. Goldstone, A. Salam and S. Weinberg, *Phys. Rev.* **127**, 965 (1962).
32. C. Itzykson and J. Zuber, *Quantum Field Theory* (McGraw-Hill, New York, 1980).
33. E. Del Giudice, S. Doglia, M. Milani and G. Vitiello, *Nucl. Phys. B* **251**(FS 13), 375 (1985).
34. E. Del Giudice, S. Doglia, M. Milani and G. Vitiello, *Nucl. Phys. B* **275**(FS 17), 185 (1986).
35. H. Matsumoto, N. J. Papastamatiou, H. Umezawa and G. Vitiello, *Nucl. Phys. B* **97**, 61 (1975).
36. H. Matsumoto, N. J. Papastamatiou and H. Umezawa, *Nucl. Phys. B* **97**, 90 (1975).
37. H. Umezawa, *Advanced Field Theory: Micro, Macro and Thermal Concepts* (AIP, New York, 1993).
38. H. Umezawa, M. Matsumoto and M. Tachiki, *Thermo Field Dynamics and Condensed States* (North-Holland, Amsterdam, 1982).
39. E. Alfinito and G. Vitiello, *Int. J. Mod. Phys. B* **14**, 853 (2000). [*Erratum-ibid. B* **14**, 1613 (2000)].
40. E. Alfinito, O. Romei and G. Vitiello, *Mod. Phys. Lett. B* **16**, 93 (2002).
41. E. Alfinito and G. Vitiello, *Phys. Rev. B* **65**, 054105 (2002).
42. P. W. Anderson, *Basic Notions of Condensed Matter Physics* (Benjamin, Menlo Park, 1984).
43. P. Higgs, *Phys. Rev.* **145**, 1156 (1966).
44. T. W. B. Kibble, *Phys. Rev.* **155**, 1554 (1967).
45. W. J. Freeman and J. Zhai, *Cogn. Neurodyn.* **3**(1), 97 (2009); http://repositories.cdlib.org/postprints/3374.
46. L. M. A. Bettencourt, N. A. Antunes and W. H. Zurek, *Phys. Rev. D* **62**, 065005 (2000).
47. N. A. Antunes, L. M. A. Bettencourt and W. H. Zurek, *Phys. Rev. Lett.* **82**, 2824 (2000).
48. M. Hindmarsh and A. Rajantie, *Phys. Rev. Lett.* **85**, 4660 (2000).
49. A. M. Perelomov, *Generalized Coherent States and their Applications* (Springer, Berlin, 1986).
50. R. Manka and G. Vitiello, *Ann. Phys.* **199**, 61 (1990).
51. T. W. B. Kibble, in *Topological Defects and the Non-equilibrium Dynamics of Symmetry Breaking Phase Transitions*, NATO Science Series C, Vol. 549, eds. Y. M. Bunkov and H. Godfrin (Kluwer Acad., Dordrecht, 2000), p. 7.
52. G. E. Volovik, in *Topological Defects and the Non-equilibrium Dynamics of Symmetry Breaking Phase Transitions*, NATO Science Series C, Vol. 549, eds. Y. M. Bunkov and H. Godfrin (Kluwer Acad., Dordrecht, 2000), p. 353.
53. W. H. Zurek, *Phys. Rep.* **276**, 177 (1997) and refs. therein quoted.
54. R. Kozma, Unpublished data (2005).
55. R. Jackiw, *Rev. Mod. Phys.* **49**, 681 (1977).
56. G. Vitiello, *My Double Unveiled* (John Benjamins, Amsterdam, 2001).
57. D. Cangemi, R. Jackiw and B. Zwiebach, *Ann. Phys.* **245**, 408 (1996).
58. E. Celeghini, M. Rasetti and G. Vitiello, *Ann. Phys.* **215**, 156 (1992).
59. G. Vitiello, in *Quantum Analogues: From Phase Transitions to Black Holes and Cosmology*, Lectures Notes in Physics, Vol. 718, eds. W. G. Unruh and R. Schuetzhold (Springer, Berlin, 2007).
60. W. J. Freeman, S. O'Nuillain and J. Rodriguez, *J. Integrative Neurosci* **7**(3), 337 (2008); http://repositories.cdlib.org/postprints/3373.
61. W. J. Freeman and B. C. Burke, *Int. J. Bifurc. Chaos* **13**, 2857 (2003).

62. M. E. Raichle, *Science* **314**, 1249 (2006).
63. G. Vitiello, *New Mathematics and Natural Computing* **5**, 245 (2009).
64. G. Vitiello, Fractals and the Fock-Bargmann representation of coherent states, in *Quantum Interaction. Third International Symposium (QI-2009)*, Saarbruecken, Germany, eds. P. Bruza, D. Sofge, *et al.* Lecture Notes in Artificial Intelligence, eds. R. Goebel, J. Siekmann and W. Wahlster (Springer-Verlag, Berlin Heidelberg, 2009), pp. 6–16.
65. M. Heidegger, *The Basic Problems of Phenomenology* (rev. ed.). Hofstadter A (trans.) Indiana UP, Bloomington, IN, 1975/1988.
66. G. Vitiello, *Int. J. Mod. Phys. B* **18**, 785 (2004).
67. E. Pessa and G. Vitiello, *Mind and Matter* **1**, 59 (2003).
68. E. Pessa and G. Vitiello, *Int. J. Mod. Phys. B* **18**, 841 (2004).
69. C. De Concini and G. Vitiello, *Nucl. Phys. B* **116**, 141 (1976).
70. B. Haider, A. Duque, A. R. Hasenstaub and D. A. McCormick, *J. Neurosci.* **26**, 4535 (2006).
71. C. C. Peterson, T. T. G. Hahn, M. Mehta, A. Grinvald and B. Sakmann, *Proc. Natl. Acad. Sci. USA* **100**, 13638 (2003).